INFLUENCE OF CONDUCTING PLATE BOUNDARY CONDITIONS ON THE RMS ENVELOPE EQUATIONS DESCRIBING INTENSE ION BEAM TRANSPORT*

Steven M. Lund, Lawrence Livermore National Laboratory, Livermore, CA 94550
Boris Bukh, Lawrence Berkeley National Laboratory, Berkeley, CA 94720

Abstract

In typical diagnostic applications, intense ion beams are intercepted by a conducting plate with slits to measure beam phase-space projections. This results in the transverse space-charge field near the plate being shorted out, rendering simple envelope models with constant space-charge strength inaccurate. Here we develop a simple corrected envelope model based on analytical calculations to account for this effect on the space-charge term of the envelope equations, enabling more accurate comparisons with experiment. Results are verified with 3D self-consistent PIC simulations.

INTRODUCTION

Low-order models of intense ion beams often employ the rms envelope equations to describe the self-consistent evolution of the beam edge in response to applied focusing, space-charge, and thermal defocusing forces.[1] Such envelope models are typically solved with constant beam emittances (phase-space area) and perveance (space-charge strength) to extrapolate experimental measurements and understand the evolution of the beam envelope away from diagnostic stations. Developing a simple model to compensate for changes in the envelope induced by plates used in diagnostics is important to enable more precise estimates of the beam envelope without the need for large simulations. Elimination of systematic errors in this process improves beam envelope control and matching — important to limit the generation of beam halo and related particle losses.

ENVELOPE MODEL

Consider a long-pulse, unbunched beam with particles of charge q and mass m moving with axial velocity $\beta_b c$ and relativistic factor $\gamma_b = 1/\sqrt{1-\beta_b^2}$. We take the transverse orbit $x(s)$ of a beam particle to satisfy the paraxial (axial energy variation of particles neglected) equation of motion[1]

$$x'' + \kappa_x x + \frac{q}{m\gamma_b^3\beta_b^2 c^2}\frac{\partial \phi}{\partial x} = 0. \qquad (1)$$

Here, s is the axial coordinate of a beam slice, $\kappa_x(s)$ is the linear applied focusing functions of the lattice, and the electrostatic potential ϕ is related to the density of beam particles n by the 3D Poisson equation $\nabla^2\phi = -qn/\epsilon_0$ subject to $\phi =$ const on conducting boundaries. An analogous equation applies to the y-orbit $y(s)$.

Denote a transverse statistical average in a axial slice of beam particles by $\langle \cdots \rangle_\perp$. RMS measures of the transverse edge radii of the beam envelope are

$$r_x(s) = 2\sqrt{\langle x^2\rangle_\perp} \quad \text{and} \quad r_y(s) = 2\sqrt{\langle y^2\rangle_\perp}. \qquad (2)$$

Differentiating the equation for r_x and employing Eq. (1) yields the envelope equation

$$r_x'' + \kappa_x r_x - \frac{2Q}{r_x + r_y}F_x - \frac{\epsilon_x^2}{r_x^3} = 0. \qquad (3)$$

Here, $Q = q\lambda/(2\pi\epsilon_0 mc^2\gamma_b^3\beta_b^2) =$ const is the dimensionless perveance ($\lambda =$ const is the line-charge density of the beam slice),

$$F_x = -\frac{4\pi\epsilon_0}{\lambda}\left(\frac{r_x + r_y}{r_x}\right)\left\langle x\frac{\partial\phi}{\partial x}\right\rangle_\perp, \qquad (4)$$

is a form-factor, and

$$\varepsilon_x = 4\left[\langle x^2\rangle_\perp\langle x'^2\rangle_\perp - \langle xx'\rangle_\perp^2\right]^{1/2} \qquad (5)$$

is the rms emittance. Analogous equations to (3)–(5) apply in y. For the special case of 2D ($\partial/\partial z = 0$) transverse self-fields with constant charge density on nested elliptical surfaces with principal axis radii αr_x and αr_y aligned with the x- and y-coordinate axes, Sacherer[2] showed that $F_x = F_y = 1$. The Vlasov model self-consistent KV distribution satisfies this condition for a uniform density elliptical beam with $\epsilon_x =$ const and $\epsilon_y =$ const. The envelope equations (3) are also often applied with $F_x = F_y = 1$ in an rms equivalent beam sense.[1,2]

SELF-FIELD SOLUTION

We model a beam near a conducting plate as impinging on a perfectly conducting plane at $z = 0$ in free-space from $z < 0$. Then the method of images can be used to solve for ϕ in the beam region with $z < 0$ as

$$\phi(\mathbf{x}) = \frac{q}{4\pi\epsilon_0}\int_{\text{beam}} d^3\tilde{x}\,\left[\frac{n(\tilde{\mathbf{x}})}{|\mathbf{x}-\tilde{\mathbf{x}}|} - \frac{n(\tilde{\mathbf{x}}_I)}{|\mathbf{x}-\tilde{\mathbf{x}}_I|}\right], \qquad (6)$$

where $\mathbf{x} = x\hat{\mathbf{x}} + y\hat{\mathbf{y}} + z\hat{\mathbf{z}}$ and $\mathbf{x}_I = x\hat{\mathbf{x}} + y\hat{\mathbf{y}} - z\hat{\mathbf{z}}$ are the direct and image coordinates, and we have dropped an arbitrary additive constant. We further idealize by assuming that the beam is normally incident with uniform density and a constant, round edge-radius ($r_x = r_y = R =$ const). Then the beam density is

$$n(r,z) = \frac{\lambda}{\pi q R^2}\Theta(R-r)\Theta(-z), \qquad (7)$$

*This research was performed at LLNL and LBNL under US DOE contact Nos. W-7405-Eng-48 and DE-AC03-76SF0098.

where $\Theta(x)$ is the Heaviside step-function [$\Theta(x) = 0$ for $x < 0$ and $\Theta(x) = 1$ for $x > 0$]. In (r, θ, z) cylindrical coordinates, $1/|\mathbf{x} - \tilde{\mathbf{x}}|$ can be expanded as[3]

$$\frac{1}{|\mathbf{x} - \tilde{\mathbf{x}}|} = \sum_{m=-\infty}^{\infty} \int_0^{\infty} dk\, e^{im(\theta - \tilde{\theta})} J_m(kr) J_m(k\tilde{r}) e^{k(z_> - z_<)},$$

where $z_>$ and $z_<$ denote the greater and lesser of z and $\tilde{z}$, and $J_m(x)$ is an mth-order ordinary Bessel function. Using this expansion and Eq. (7) in Eq. (6) gives in the beam

$$\phi(r,z) = \frac{\lambda}{\pi\epsilon_0} \int_0^{\infty} \frac{dw}{w^2} \left(1 - e^{-w|z|/R}\right) J_0\left(w\frac{r}{R}\right) J_1(w),$$

and the corresponding radial and axial electric field components $E_r = -\partial\phi/\partial r$ and $E_z - -\partial\phi/\partial z$ are

$$E_r(r,z) = \frac{\lambda}{\pi\epsilon_0 R} \int_0^{\infty} \frac{dw}{w} \left(1 - e^{-w|z|/R}\right) J_1\left(w\frac{r}{R}\right) J_1(w),$$

$$E_z(r,z) = \frac{\lambda}{\pi\epsilon_0 R} \int_0^{\infty} \frac{dw}{w}\, e^{-w|z|/R} J_0\left(w\frac{r}{R}\right) J_1(w). \qquad (8)$$

These field components are plotted in Fig. 1. Note that the radial field remains nearly linear within the beam ($r < R$) until z is a fraction of a beam radius from the plate. The axial field increases near the plate because the negative image beam is closer.

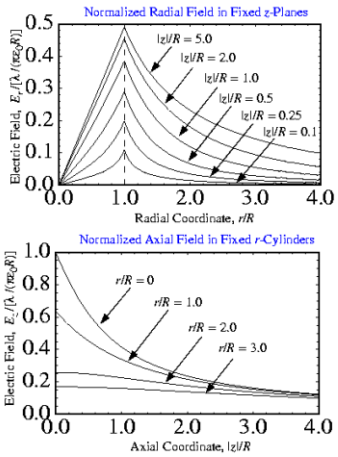

FIG. 1: Self-field components near a conducting plate.

Equations (8) are checked by calculating the limits

$$\lim_{z\to-\infty} E_r(r,z) = \frac{\lambda}{\pi\epsilon_0 R} \int_0^{\infty} \frac{dw}{w} J_1\left(w\frac{r}{R}\right) J_1(w)$$

$$= \frac{\lambda}{2\pi\epsilon_0 R} \cdot \begin{cases} \frac{r}{R}, & 0 \le \frac{r}{R} \le 1, \\ \frac{1}{r/R}, & 1 \le \frac{r}{R}, \end{cases}$$

$$E_z(r=0,z) = \frac{\lambda}{\pi\epsilon_0 R} \int_0^{\infty} \frac{dw}{w}\, e^{-w|z|/R} J_1(w)$$

$$= \frac{\lambda}{\pi\epsilon_0 R^2} \left(\sqrt{R^2 - z^2} - |z|\right). \qquad (9)$$

The radial field limit is the usual expression for a uniform density beam of radius R. The axial field limit shows that $\phi(r = 0, z)$ logarithmically diverges in $|z|$. This divergence is related to the 2D nature of the problem and shows that this model is inadequate for direct use in estimates of axial acceleration induced by the plate. Regularization of this divergence to model image induced self-field accelerations can be carried out by adding a grounded, cylindrical pipe to cutoff the self-field interaction range (as would be present in the laboratory).

CORRECTED AXISYMMETRIC ENVELOPE EQUATION

We apply the self-field solution above to motivate a simple, corrected envelope equation for an axisymmetric beam with a normally incident centroid impinging on a conducting plate from $z < 0$. We take $\kappa_x(s) = \kappa_y(s) \equiv \kappa(s)$, $\epsilon_x = \epsilon_y \equiv \epsilon$, and $r_x(s) = r_y(s) \equiv R(s)$. The form-factors (4) are calculated from Eq. (8) as

$$F_x = F_y = -\frac{4\pi\epsilon_0}{\lambda} \left\langle r\frac{\partial\phi}{\partial r} \right\rangle_{\perp} = F\left(\frac{|z|}{R}\right) \qquad (10)$$

where,

$$F(\zeta) \equiv 8 \int_0^{\infty} \frac{dw}{w^2} \left(1 - e^{-w\zeta}\right) J_1(w) J_2(w). \qquad (11)$$

We apply this form-factor to a beam with evolving radius $r_x(s) = r_y(s) = R(s)$ to obtain a corrected axisymmetric beam envelope equation

$$R'' + \kappa\, R - \frac{Q}{R} F\left(\frac{|s - s_p|}{R}\right) - \frac{\varepsilon^2}{R^3} = 0. \qquad (12)$$

Here, $|s - s_p|$ is the axial distance of the beam slice from the conducting plate.

An approximate analytical expression for the form-factor (11) can be calculated using the on-axis field $E_z(r = 0, z)$ in Eq. (9) and the Poisson equation to derive a power series solution for E_r valid within the beam. Truncating this series to radial terms of order r^3 and lower yields

$$F(\zeta) \simeq \frac{\zeta}{\sqrt{1+\zeta^2}} \left[1 + \frac{1}{4}\frac{1}{1+\zeta^2}\left(1 - \frac{\zeta^2}{1+\zeta^2}\right)\right]. \qquad (13)$$

The "exact" [Eq. (11)] and approximate [Eq. (13)] form-factors are plotted versus ζ in Fig. 2. For large ζ note that $F \simeq 1$ and we obtain the usual envelope equations, whereas F rapidly decreases to zero for ζ corresponding to several beam radii from the plate where the radial self-field is shorted out by the conducting plate, thereby decreasing the strength of the perveance term in the envelope equation.

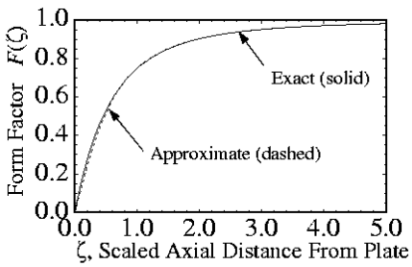

FIG. 2: Form factor and approximate form factor.

A numerical solution to the corrected envelope equation (12) is plotted in Fig. 3 together with the uncorrected solution for $F = 1$. Parameters correspond to typical diagnostic situations in the High Current Experiment (HCX) for Heavy-Ion Fusion (HIF),[4] where a 1–1.8 MeV, 200–700 mA, K^+ ion-beam with $\varepsilon_x \sim \varepsilon_y \sim$ 50–100 mm-mrad is

Perveance	Emittance	Initial conditions		Final Conditions (R in mm, R' in mrad)					
Q	ε	$R(0)$	$R'(0)$	$F=1$		$F=F(\lvert s-s_p\rvert/R)$		3D PIC Simulation	
	(mm-mrad)	(cm)	(mrad)	$R(s_p)$	$R'(s_p)$	$R(s_p)$	$R'(s_p)$	$R(s_p)$	$R'(s_p)$
$8.\cdot10^{-4}$	100.	1.	0.	1.0220	6.2444	1.0211	5.5765	1.0223	5.5508
$8.\cdot10^{-4}$	100.	1.	20.	1.1608	25.7757	1.1600	25.1224	1.1616	25.1150
$8.\cdot10^{-4}$	100.	1.	40.	1.2998	45.3919	1.2990	44.7511	1.3012	44.7790
$8.\cdot10^{-4}$	100.	1.	$-20.$	0.8833	-13.1644	0.8825	-13.8492	0.8836	-13.8960
$8.\cdot10^{-4}$	100.	1.	$-40.$	0.7450	-32.3841	0.7442	-33.0866	0.7448	-33.1350
$10.\cdot10^{-4}$	50.	1.	0.	1.0250	7.1132	1.0212	5.5765	1.0178	5.2704
$10.\cdot10^{-4}$	50.	1.	20.	1.1639	26.6470	1.1600	25.1224	1.1567	24.8105
$10.\cdot10^{-4}$	50.	1.	$-20.$	0.8863	-12.3204	0.8825	-13.8492	0.8791	-14.1640

TABLE I: Initial and final envelope radii and angles for uncorrected and corrected envelope models and self-consistent PIC simulations.

focused in a FODO quadrupole lattice with period 60 cm and an undepressed particle phase advance of $\sigma_0 = 60°$–$90°$. Free-drifts to diagnostic stations are $\sim$ 7 cm, average matched beam radii are $\sim$ 1 cm, and maximum matched beam envelope angles are $\sim$ 50 mrad. Final values of envelope solutions for a range of HCX-like parameters are contrasted in Table I for form-factors $F = 1$ and $F(|s - s_p|/R)$. The most significant correction for these parameters is in the envelope angle at the plate $R'(s_p)$ with typical experimentally resolvable errors $\sim$ 1 mrad occurring. Envelope coordinate errors $R(s_p)$ are not resolvable.

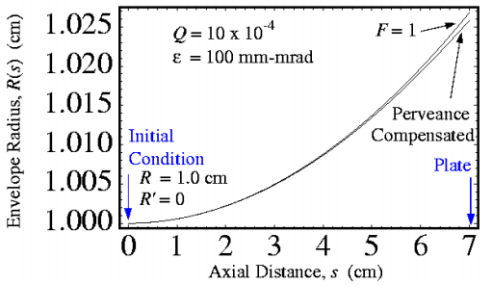

FIG. 3: Envelope for a drift solution into a plate.

PIC SIMULATIONS

Self-consistent 3D electrostatic PIC simulations were carried out to check the corrected envelope model predictions presented above for deviations due to: self-field nonlinearities, emittance growth, variation in the beam envelope near the plate [$R(s) \neq$ const in beam self-fields], energy deviations due to the beam seeing it's image in the plate, and elliptical beam effects due to $r_x \neq r_y$ (simulated but not presented in this article). The WARP code developed by LLNL for simulation of intense beams for HIF applications was employed. This code is modular with an extensive hierarchy of models.[5] We carried out simulations with: a 10 cm radial beam pipe with $\phi = 0$, boundary conditions on the left and right axial bounds with $E_z = 0$ (at injection) and $\phi = 0$ (at plate), and steady-state mid-pulse solutions iterated from uniform, semi-Gaussian beam injection conditions on the left axial boundary. Results of these simulations are included in Table I and agree well with corrected envelope model results for typical ranges of Q in the HCX experiment.[4] The simulations showed negligible rms emittance growth ($\sim 1\%$ and less) and verified that the nonlinear space-charge fields within a fraction of a beam radius of the plate have insufficient time to cause deviations from the simple envelope model.

CONCLUSIONS

Generalized transverse envelope equations were derived to improve modeling of intense ion-beams impinging at normal incidence on a conducting plate. These equations were analyzed in an axisymmetric limit using an analytical solution form-factor to account for the plate shorting-out the space-charge field near the plate. Model results compared well with self-consistent 3D PIC simulations. Contrasting results with standard (fixed perveance term) envelope equations for usual parameters shows that small, but significant angle errors result if this effect is not corrected. Comparisons of experimental results to envelope models were improved by incorporating this systematic effect in the analysis of the HCX experiment. In this work, we employed heuristic form-factors to model the experimental beam with elliptical cross-section:

$$F_x = F_y = F\left(\frac{|s-s_p|}{\sqrt{r_x(s)r_y(s)}}\right). \qquad (14)$$

Simulations verify that this replacement recovers most of the correction for elliptical beams without extreme ellipticity ($r_x/r_y \sim 3$ and less) and in continuing studies we are developing improved approximations.

ACKNOWLEDGMENTS

The authors wish to thank Edward Lee and John Barnard for useful discussions and Dave Grote and Jean-Luc Vay for help with the WARP simulations.

REFERENCES

1. M. Reiser, *Theory and Design of Charged Particle Beams*, (Wiley, 1994).
2. F.J. Sacherer, IEEE Trans. Nuc. Sci. **14**, 1105 (1971).
3. J.D. Jackson, *Classical Electrodynamics*, (Wiley, 1975).
4. P.A. Seidl et al., paper ROAC001, PAC 03.
5. D.P. Grote, et al., Nuc. Instr. Meth. A **415**, 428 (1998).